Applications of Cumulants to Array Processing—Part IV: Direction Finding in Coherent Signals Case

Egemen Gönen, Jerry M. Mendel, *Fellow, IEEE*, and Mithat C. Doğan, *Member, IEEE*

***Abstract*— We present a subspace-based direction-finding method for coherent signal environments using an antenna array. Our method, which uses fourth-order statistics, is capable of resolving more signals than a comparable second-order statistics-based subspace method and is applicable to a larger class of arrays. The maximum number of signals resolvable with our method may exceed the number of sensors in the array. Only a uniform linear subarray is needed; the rest of the array may have arbitrary and unknown response and does not require calibration. On the other hand, the comparable second-order statistics-based method is limited to uniform linear arrays only. No search procedure is needed in our method. Simulation experiments supporting our conclusions are provided.**

***Index Terms*—Array processing, coherent signals, cumulants, direction finding, higher order statistics, multipath propagation.**

I. INTRODUCTION

HIGHLY correlated or coherent signals are often the case in multipath propagation environments or in military scenarios when there are smart jammers. Existing second-order-statistics-based subspace methods for direction finding fail in coherent signal environments. To handle the coherency problem, some solutions were proposed [1], [5], [9], [13], [15]–[17]; however, these solutions are either limited to specific array configurations, or unreasonable assumptions were made. For example, the *spatial smoothing method* of [15] and [16] is limited to uniform linear arrays and results in a smaller number of resolved signals than that which can be resolved with the same array under the absence of coherence; the solution presented in [1] and [17] requires computationally intense multidimensional search, and [9] proposes using moving arrays. Additionally, in [5], an attempt was made to generalize spatial smoothing to a class of arbitrary but very restrictive array geometries by using interpolated arrays; however, it was assumed that the array manifold is known, which requires calibration of the entire array. Porat and Friedlander present a modified version of their cumulant-based algorithm [13] to handle the case of coherent signals; however, their method is not practical because it requires selection of a highly redundant subset of fourth-order cumulants that contains $O(N^4)$ elements, and no guidelines exist for its selection; Second-, fourth-, sixth-, and eighth-order moments of the data are required. We have shown [8] that using cumulants, the case of coherent signals can be handled without calibration and with a weaker constraint on the array structure than required by the second-order statistics-based methods.

For independent signals, Doğan and Mendel [2] have developed the virtual-ESPRIT algorithm (VESPA) for direction finding. It is based on their virtual cross-correlation computer (VC^3). VESPA can calibrate an array of unknown configuration and arbitrary response by using just one additional pair of identical sensors (instead of a copy of the entire array or storage of the entire array response for every possible scenario, which is required by ESPRIT).

In this paper, we extend VESPA to the case of coherent signals. Our method, which we will refer to as *extended VESPA* (EVESPA) throughout the paper, is capable of resolving more signals than the second-order-statistics-based spatial smoothing method and is applicable to a larger class of arrays. The number of resolvable signals may exceed the number of sensors in our method. Only a uniform linear subarray is needed; the rest of the array may have arbitrary and unknown response and does not require calibration. On the other hand, the spatial smoothing method is limited to uniform linear arrays.

In Section II, we define the problem. A solution to the problem is presented in Section III. Section IV explains how the available data can be used more efficiently. Results of simulation experiments are provided in Section V. Conclusions are in Section VI.

Throughout the paper, lower-case boldface letters represent vectors; upper-case boldface letters represent matrices; and lower and upper-case letters represent scalars. $\boldsymbol{C}(i, j)$ represents the ijth element of the matrix $\boldsymbol{C}$. The symbol "*" is used for conjugation operation, and the superscript "^{H}" is used to denote complex conjugate transpose.

II. FORMULATION OF THE PROBLEM

In order to describe the problem best, a summary of VESPA will be presented first. Then, we will explain why VESPA fails in the coherent signals case. To show the interconnection

Manuscript received May 6, 1996; revised March 4, 1997. This work was supported by the Center for Research on Applied Signal Processing at the University of Southern California. The associate editor coordinating the review of this paper and approving it for publication was Prof. Michael D. Zoltowski.

E. Gönen is with Globalstar L.P., San Jose, CA 95134 USA.

J. M. Mendel is with the Signal and Image Processing Institute, Department of Electrical Engineering—Systems, University of Southern California, Los Angeles, CA 90089-2564 USA.

M. C. Doğan is with the TRW Avionics and Surveillance Group, Sunnyvale, CA USA.

Publisher Item Identifier S 1053-587X(97)07054-2.

between VESPA and EVESPA for coherent signals more clearly, here, we present VESPA in a slightly different manner than is done in [2].

To begin, let us assume that P *statistically independent* narrowband signals $\{s_1(t), \cdots, s_P(t)\}$ with center frequency w_c impinge on an M-element antenna array from directions $\{\theta_1, \cdots, \theta_p\}$. Later, we will modify this to the *coherent* signals case. Assume for now that the array conforms to the VESPA model, i.e., the array antennas have arbitrary and unknown locations and responses except for two antennas that have *identical* response patterns and are cumulatively referred to as *sensor doublet*.

We will denote the signals received by the sensor doublet as $r_1(t)$ and $r_2(t)$. They are separated by $\vec{\Delta}$. Let $\boldsymbol{r}(t)$ be the snapshot vector received at time t. Then, the received signal is

$$\boldsymbol{r}(t) = \boldsymbol{A}\boldsymbol{s}(t) + \boldsymbol{n}(t) \tag{1}$$

where $\boldsymbol{A} = [\boldsymbol{a}(\theta_1), \cdots, \boldsymbol{a}(\theta_P)]$ is the $M \times P$ steering matrix in which $\boldsymbol{a}(\theta_i)$ is the response of the array to the ith signal, which is referred to as the *ith steering vector*, and $\boldsymbol{n}(t)$ is a Gaussian[1] noise process with unknown autocovariance matrix and is independent of the source signals.

VESPA starts with the estimation of two $M \times M$ fourth-order cumulant matrices $\boldsymbol{C}_1 = \text{cum}(r_1(t), r_1^*(t), \boldsymbol{r}(t), \boldsymbol{r}^H(t))$ and $\boldsymbol{C}_2 = \text{cum}(r_2(t), r_1^*(t), \boldsymbol{r}(t), \boldsymbol{r}^H(t))$ with elements

$$\begin{aligned}
\boldsymbol{C}_1(i,j) &= \text{cum}(r_1(t), r_1^*(t), r_i(t), r_j^*(t)) \\
&= \text{cum}\Bigg(\sum_{k=1}^{P} a_1(k)s_k(t), \sum_{l=1}^{P} a_1^*(l)s_l^*(t) \\
&\quad \cdot \sum_{m=1}^{P} a_i(m)s_m(t), \sum_{n=1}^{P} a_j^*(n)s_n^*(t)\Bigg) \\
&\quad + \text{cum}(n_1(t), n_1^*(t), n_i(t), n_j^*(t)) \\
&= \sum_{k=1}^{P}\sum_{l=1}^{P}\sum_{m=1}^{P}\sum_{n=1}^{P} a_1(k)a_1^*(l)a_i(m)a_j^*(n) \\
&\quad \cdot \text{cum}(s_k(t), s_l^*(t), s_m(t), s_n^*(t)) \\
&= \sum_{k=1}^{P} \gamma_{4,s_k}|a_1(k)|^2 a_i(k)a_j^*(k)
\end{aligned} \tag{2}$$

$$\begin{aligned}
\boldsymbol{C}_2(i,j) &= \text{cum}(r_2(t), r_1^*(t), r_i(t), r_j^*(t)) \\
&= \text{cum}\Bigg(\sum_{k=1}^{P} a_1(k))e^{-j\vec{k}_k\cdot\vec{\Delta}}s_k(t), \sum_{l=1}^{P} a_1^*(l)s_l^*(t) \\
&\quad \cdot \sum_{m=1}^{P} a_i(m)s_m(t), \sum_{n=1}^{P} a_j^*(n)s_n^*(t)\Bigg) \\
&\quad + \text{cum}(n_2(t), n_1^*(t), n_i(t), n_j(t)) \\
&= \sum_{k=1}^{P}\sum_{l=1}^{P}\sum_{m=1}^{P}\sum_{n=1}^{P} a_1(k)a_1^*(l)a_i(m)a_j^*(n) \\
&\quad \cdot e^{-j\vec{k}_k\cdot\vec{\Delta}}\, \text{cum}(s_k(t), s_l^*(t), s_m(t), s_n^*(t)) \\
&= \sum_{k=1}^{P} \gamma_{4,s_k}|a_1(k)|^2 e^{-j\vec{k}_k\cdot\vec{\Delta}} a_i(k)a_j^*(k)
\end{aligned} \tag{3}$$

[1] It was shown [4] that this assumption is not needed under some conditions.

where $a_i(j)$ represents the ith element of $\boldsymbol{a}(\theta_j)$; $e^{-j\vec{k}_k\cdot\vec{\Delta}} = e^{-jw_c\Delta\sin\theta_k/c}$ in which $\vec{\Delta}$ is the vector connecting the doublet's elements; $\Delta = |\vec{\Delta}|$; θ_k is measured with respect to the normal line to $\vec{\Delta}$; c is the speed of propagation of the signals, and $1 \leq i, j \leq M$. In the above derivations, cumulant properties [**CP1**], [**CP3**], [**CP5**] and [**CP6**] in [10] were used. We also used the facts that fourth-order cumulants of a Gaussian process are zero and that the first and second antennas have identical response patterns. The last lines of (2) and (3) follow from the independence of the source signals and [**CP6**], i.e.

$$\text{cum}(s_k(t), s_l^*(t), s_m(t), s_n^*(t)) = \begin{cases} \gamma_{4,s_k} & \text{if } k=l=m=n \\ 0 & \text{otherwise.} \end{cases} \tag{4}$$

Collecting (2) and (3) for $1 \leq i, j \leq M$ in matrix form, we obtain

$$\boldsymbol{C}_1 = \text{cum}(r_1^*(t), r_1(t), \boldsymbol{r}(t), \boldsymbol{r}^H(t)) = \boldsymbol{A}\boldsymbol{D}\boldsymbol{A}^{\boldsymbol{H}} \tag{5}$$

$$\boldsymbol{C}_2 = \text{cum}(r_1^*(t), r_2(t), \boldsymbol{r}(t), \boldsymbol{r}^H(t)) = \boldsymbol{A}\boldsymbol{\Phi}\boldsymbol{D}\boldsymbol{A}^{\boldsymbol{H}} \tag{6}$$

where $\boldsymbol{D} \triangleq \text{diag}\{\gamma_{4,s_1}|a_1(1)|^2, \cdots, \gamma_{4,s_P}|a_1(P)|^2\}$, and $\boldsymbol{\Phi} \triangleq \text{diag}\{e^{-jw_c\Delta\sin\theta_1/c}, \cdots, e^{-jw_c\Delta\sin\theta_P/c}\}$. For different arrival angles, $rank(\boldsymbol{A}) = rank(\boldsymbol{\Phi}) = P$, and $\boldsymbol{D}$ is full rank, provided the sources have nonzero fourth-order cumulants, and the first sensor has nonzero response to the incoming signals. With these rank conditions, (5) and (6) satisfy all the requirements of ESPRIT [14]. The last step of VESPA is to apply ESPRIT to (5) and (6) to obtain the direction of arrival estimates and steering vectors.

If the signals impinging on the array are *coherent*, covariance-based subspace direction finding methods fail because some of the signal eigenvectors diverge into the noise subspace. On the other hand, for VESPA, $rank(\boldsymbol{C}_1) = rank(\boldsymbol{C}_2) < P$, and therefore, the diagonal elements of matrix $\boldsymbol{\Phi}$ are unknown functions of both the response of array and the multipath propagation parameters. Consequently, when there are coherent signals, an explicit solution for the signal directions cannot be obtained from VESPA. In the next section, we extend VESPA to handle the coherent signals case.

III. New Solution

Consider a scenario in which there are G narrowband sources $\{u_i(t)\}_{i=1}^{G}$. Suppose that each of these signals $u_i(t)$ undergo frequency-flat multipath propagation, producing a set of delayed and scaled replicas of itself $\{s_{i,1}(t), \cdots, s_{i,p_i}(t)\}$ impinging on an M-element array from directions $\{\theta_{i,1}, \cdots, \theta_{i,p_i}\}$. In the sequel, the collection of p_i signals $\{s_{i,1}(t), \cdots, s_{i,p_i}(t)\}$, which are coherent replicas of $u_i(t)$, will be referred to as the ith *group*. Let the total number of signals impinging on the array be P, that is $\Sigma_{i=1}^{G} p_i = P$. Our assumptions are the following:

A1) The source signals $\{u_i(t)\}_{i=1}^{G}$ are statistically independent, which is a valid assumption for physically separated sources.

A2) The source signals have nonvanishing fourth-order cumulants, which is generally true for communication signals.

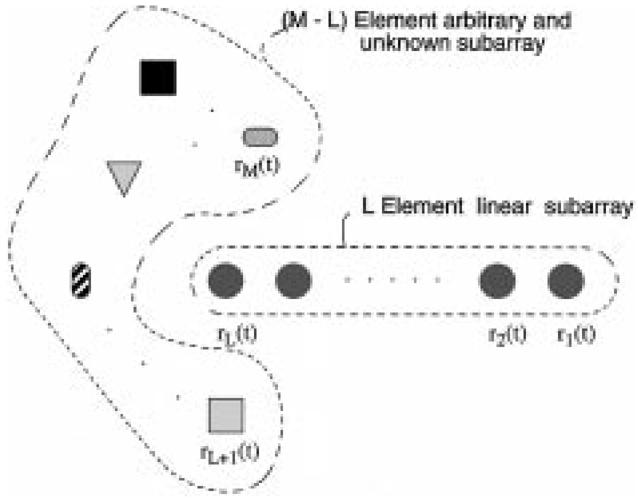

Fig. 1. Example array configuration. There are M sensors, L of which are uniform linearly positioned; $r_1(t)$ and $r_2(t)$ are identical guiding sensors. Linear subarray elements are separated by Δ.

A3) The M element array is composed of an L element uniform linear subarray and an $M-L$ element subarray having arbitrary and unknown location and response (see Fig. 1).

A4) The array is a nonambiguous one, i.e., its response to a signal from a given direction is different from that due to another signal from a different direction.

A5) The number of sources is less than the number of array elements, i.e., $G < M$). The reason for the linear subarray will be made clear below.

A6) The measurements are corrupted by additive noise, which is statistically independent of the source signals, and they can be Gaussian, non-Gaussian symmetrically distributed, or a mixture of Gaussian and this type of non-Gaussian noise.

We assume that N snapshots taken at time points $t = 1, \cdots, N$ are available. The problem is to estimate the DOA's $\{\theta_{1,1}, \cdots, \theta_{1,p_1}, \cdots, \theta_{G,1}, \cdots, \theta_{G,p_G}\}$. The solution proceeds in three steps.

A. Step 1: Estimate Generalized Steering Vectors

Assuming an unknown coherence model for the received signals, the cumulants in (5) and (6) can be written in terms of the cumulants of $\{u_i(t)\}_{i=1}^{G}$. This, in effect, permits us to separate the coherent groups, making it possible to obtain two expressions that are similar to (5) and (6).

The coherence among the received signals can be expressed as in (2) in the companion paper [7], and the received signal can then be written in terms of the independent sources as

$$\boldsymbol{r}(t) = \boldsymbol{A}\boldsymbol{s}(t) + \boldsymbol{n}(\boldsymbol{t}) = \boldsymbol{A}\boldsymbol{Q}\boldsymbol{u}(t) + \boldsymbol{n}(\boldsymbol{t}) = \boldsymbol{B}\boldsymbol{u}(t) + \boldsymbol{n}(\boldsymbol{t}) \quad (7)$$

where $\boldsymbol{A}$ is the steering matrix having columns $\boldsymbol{B} \triangleq \boldsymbol{A}\boldsymbol{Q}$, and $\boldsymbol{Q}$ is as defined in [7, eq. (2)]. Note that $\boldsymbol{B}$ is $M \times G$.

The columns of $\boldsymbol{B}$, which are referred to as the *generalized steering vectors,* can be estimated following Step 1 of the companion paper [7].

Note that $r_1(t)$ and $r_2(t)$ can be chosen as any two sensor measurements in the array, provided $\boldsymbol{D}$ and $\boldsymbol{A}$ in [7, Eqs. (4), (6)] are nonsingular. However, choosing $r_1(t)$ and $r_2(t)$ from the uniform linear subarray leads directly to the DOA estimates at this step if the signals are statistically independent because in that case, $G = P$, and $\text{diag}(B(2,1)/B(1,1), \cdots, B(2,P)/B(1,P)) = \text{diag}\{e^{-jw_c\Delta \sin\theta_1/c}, \cdots, e^{-jw_c\Delta \sin\theta_P/c}\}$, which follows from the fact that the first two sensors have identical responses. For the coherent case, however, the matrix $\boldsymbol{D}$ does not give the DOA's explicitly; however, the estimated generalized steering vectors can be used to find the DOA's, as explained in the next step.

B. Step 2: Spatial Smoothing

Once we have estimated the generalized steering vectors $\{\boldsymbol{b}_i\}_{i=1}^{G}$, we can estimate the steering vector and, subsequently, the DOA of each signal path. The general form of coherence between the received signals lets us express each generalized steering vector as a linear combination of steering vectors of *one* coherent group, *independent* of the other steering vectors, where the combination coefficients are the elements of the *unknown* complex propagation vector for that group. To see this, partition the matrices $\boldsymbol{B}$ and $\boldsymbol{A}$ as $\boldsymbol{B} = [\boldsymbol{b}_1, \cdots, \boldsymbol{b}_G]$ and $\boldsymbol{A} = [\boldsymbol{A}_1, \cdots, \boldsymbol{A}_G]$, where $\boldsymbol{b}_i$ is $M \times 1$, and the steering matrix for the ith group $\boldsymbol{A}_i \triangleq [\boldsymbol{a}(\theta_{i,1}), \cdots, \boldsymbol{a}(\theta_{i,p_i})]$ is $M \times p_i$. Additionally, $\theta_{i,m}$ represents the angle of arrival of the mth signal in the ith coherent group with $1 \leq m \leq p_i$. Using the fact that the ith column of $\boldsymbol{Q}$ in (2) of [7] has p_i nonzero elements, $\boldsymbol{B}$ can be expressed as $\boldsymbol{B} = \boldsymbol{A}\boldsymbol{Q} = [\boldsymbol{A}_1\boldsymbol{c}_1, \cdots, \boldsymbol{A}_G\boldsymbol{c}_G]$; therefore, the ith column of $\boldsymbol{B}, \boldsymbol{b}_i$ is $\boldsymbol{b}_i = \boldsymbol{A}_i\boldsymbol{c}_i$ where $i = 1, \cdots, G$.

Now, the problem of solving for steering vectors of the received signals is transformed into G independent problems, each solving for the steering vectors of all the signal paths in each coherent group from the generalized steering vector of that group. To solve each of these new problems, each generalized steering vector $\boldsymbol{b}_i$ can be interpreted as a received signal for an array illuminated by p_i coherent signals having a steering matrix $\boldsymbol{A}_i$, and covariance matrix $\boldsymbol{c}_i\boldsymbol{c}_i^H$. Then, the DOA's of each signal could be solved for by using a second-order-statistics-based subspace method such as MUSIC if the array is calibrated and if the rank of $\boldsymbol{c}_i\boldsymbol{c}_i^H$ is p_i; however, the array is not calibrated, and $\text{rank}(\boldsymbol{c}_i\boldsymbol{c}_i^H) = 1$. Therefore, we propose to keep only the part of each estimated generalized steering vector that corresponds to the *linear* part of the array. By doing this, we will be able to incorporate spatial smoothing [12], [15], which, in turn, will *restore* the rank of $\boldsymbol{c}_i\boldsymbol{c}_i^H$ to p_i.

For this purpose, partition $\boldsymbol{b}_i$ as

$$\boldsymbol{b}_i = \begin{bmatrix} \boldsymbol{b}_{L,i} \\ \boldsymbol{b}_{M-L,i} \end{bmatrix} = \begin{bmatrix} \boldsymbol{A}_{L,i} \\ \boldsymbol{A}_{M-L,i} \end{bmatrix} \boldsymbol{c}_i \quad (8)$$

for $i = 1, \cdots, G$, where $\boldsymbol{b}_{L,i}$ is the portion of $\boldsymbol{b}_i$ corresponding to the uniform linear subarray of sensors (the first L elements of $\boldsymbol{b}_i$ for the array configuration in Fig. 1), and $\boldsymbol{A}_{L,i}$ contains the first L rows of $\boldsymbol{A}_i$. Now, $\boldsymbol{b}_{L,i}$ can be interpreted [8] as a received signal for an L-element uniform linear array that is illuminated by coherent signals from a *single* source whose propagation vector is $\boldsymbol{c}_i$. Note that the steering matrix of these coherent signals is $\boldsymbol{A}_{L,i}$. Treating $\boldsymbol{b}_{L,i}\boldsymbol{b}_{L,i}^H$ as the covariance matrix of the received signal, spatial smoothing can be applied to restore the rank of $\boldsymbol{b}_{L,i}\boldsymbol{b}_{L,i}^H$ to p_i for $i = 1, \cdots, G$, and then, any second-order-statistics-based high-resolution method can be employed to find the DOA's. Note that the antenna patterns of the sensors in the uniform linear subarray, which are the same, are not required, i.e., calibration is not needed.

Forward spatial smoothing [12], [15] for the ith group $(i = 1, \cdots, G)$ starts by dividing the L-vector $\boldsymbol{b}_{L,i}$ into $K = L - S + 1$ overlapping subvectors of size $S, \boldsymbol{b}_{S,i}^k$ $(k = 1, \cdots, K)$, with elements $\{b_{L,i}(k), \cdots, b_{L,i}(k+S-1)\}$. Then, a forward spatially smoothed matrix $\overline{\boldsymbol{b}_{S,i}\boldsymbol{b}_{S,i}^H}$ is calculated as

$$\overline{\boldsymbol{b}_{S,i}\boldsymbol{b}_{S,i}^H} = \frac{1}{K}\sum_{k=1}^{K} \boldsymbol{b}_{S,i}^k \boldsymbol{b}_{S,i}^{k\ H}. \tag{9}$$

The conditions on the length of the linear subarray and the parameter S under which the rank of $\boldsymbol{b}_{S,i}\boldsymbol{b}_{S,i}^H$ is restored to p_i are as follows [6]:

L must satisfy $L \geq 2p_i$ if forward spatial smoothing is used, and $L \geq 3p_i/2$ if both forward and backward smoothing are used [12]. This means that if both methods are used, the linear subarray must have at least $3p_{\max}/2$ elements, where $p_{\max}$ is the maximum number of multipaths in anyone of the G groups. Given L and $p_{\max}$, the parameter S must be selected such that $p_{\max} + 1 \leq S \leq L - p_{\max}/2 + 1$.

C. Step 3: Extract DOA's

By applying any second-order-statistics-based subspace technique (e.g., root-MUSIC, etc.) to the pseudo-covariance matrix $\overline{\boldsymbol{b}_{S,i}\boldsymbol{b}_{S,i}^H}, i = 1, \cdots, G$, it is possible to estimate DOA's of up to $2L/3$ coherent signals in each group. As just noted, a linear subarray of minimum dimension $3p_{\max}/2$ is needed.

D. Discussion

Since $\boldsymbol{B}$ is $M \times G$, the maximum number of groups G that can be resolved is $M - 1$. Additionally, as we have just seen, it is possible to estimate DOA's of up to $2L/3$ coherent signals in each group. Consequently, the maximum total number of coherent signals that can be resolved by our method is $2(M-1)L/3$. If all sensors are in a uniform linear array $(M = L)$, then a maximum of $2(M-1)M/3$ coherent signals can be resolved.

Note that in deriving our three-step method, we did not restrict the entire array to be linear. Only an L-element part of it must be linear. In contrast, when the signals are coherent, second-order-statistics-based methods using spatial smoothing [12], [15] are limited to uniform linear arrays. In addition, given an L-element uniform linear array, while our method can resolve at most $2(L-1)L/3$ signals, these methods can resolve at most $L - 1$ signals. This clearly demonstrates the increased resolving capacity of our method.

Another point to note is that if a coherent group contains more than $2L/3$ signals, only the DOA estimates of that group are affected because each group is treated *independently* in the second step of our method.

Finally, even if there are no multipaths, our method works because in this case, spatial smoothing does not affect the unity rank of $\boldsymbol{b}_{S,i}\boldsymbol{b}_{S,i}^H$ since there is only one signal in the ith group. Note that our method works for coherent or linearly correlated signals as well as independent signals. On the other hand, VESPA works only for the independent signals case. The tradeoff from a hardware standpoint is that our method requires a uniform linear subarray whose length depends on the number of multipaths in a coherent group, whereas VESPA requires two identical sensors. If one suspects any multipath will be present in the data, EVESPA must be used.

IV. Efficient Use of Data

In this section, we show that our method can be modified to use the available data more efficiently.

A. Using Multiple Guiding Sensor Pairs

Just as when we chose the first two sensors as the guiding pair, the two pairs of sensors (m, p) and $(m, q), p \neq q$ also lead to two matrices, like [7, (4), (6)], which are in ESPRIT form to estimate the generalized steering vectors $\{\boldsymbol{b}_{L,1}, \cdots, \boldsymbol{b}_{L,G}\}$. On the other hand, VESPA requires guiding sensor pair elements to have identical responses because VESPA is based on the fact that responses of *identical* but displaced sensors are identical up to a phase constant that contains the angle of arrival information. Consequently, we have more degrees of freedom in our method than in VESPA. This observation suggests that the available data can be used efficiently by employing multiple guiding sensor pairs in Step 1, as explained in Section III-D of the companion paper [7]. Since the required computations for different choices of guiding sensor pairs are independent, they can be implemented in *parallel*. However, as mentioned in [7], we have found that using multiple guiding sensor pairs does not lead to substantial improvements to warrant the extra computations.

B. Using Covariance Information

Sensor-to-sensor independence of the measurement noise lets us use the spatial covariance matrix of the array as side information to improve the generalized steering vector estimates and bearing estimates in our method. If it is known that the measurement noise is spatially white, the eigenvectors of the spatial covariance matrix corresponding to the smallest repeated eigenvalues span the noise subspace, and the remaining eigenvectors define the signal subspace.

Although we cannot identify the generalized steering vectors from the covariance matrix when coherence is present, we can improve our cumulant-based steering vector estimates by projecting them onto the signal subspace obtained from the spatial covariance matrix [2]. As explained in [2], the motivation behind this approach is that the variance of covariance estimates is lower than that of cumulant estimates for the same sample size. Note that this method is applicable only if the noise is white.

If the goal is to estimate the DOA's, we proceed to improve our generalized steering vector estimates in EVESPA by

1) estimating the spatial covariance matrix corresponding to the uniform linear part of the array;
2) identifying the signal subspace eigenvectors by eigenanalysis of the spatial covariance matrix;
3) stacking the signal subspace eigenvectors into an $L \times G$ matrix $\boldsymbol{E}_s$ (if there are G coherent groups, the signal subspace is G dimensional);
4) projecting the cumulant-based generalized steering vector estimates $\{\boldsymbol{b}_{L,i}\}_{i=1}^{G}$ onto the signal subspace to obtain improved estimates $\{\boldsymbol{b}_{L,i,\text{imp}}\}_{i=1}^{G}$, i.e., $\boldsymbol{b}_{L,i,\text{imp}} = \boldsymbol{E}_s\boldsymbol{E}_s^H\boldsymbol{b}_{L,i}$. These improved generalized steering vector estimates are used in the spatial smoothing step of EVESPA.

C. Improving the Generalized Steering Vector Estimates by Beamforming

The quality of bearing estimates in each coherent group depends on the accuracy of the corresponding generalized steering vector estimates. Although different groups are statistically independent, cross-term effects are present in the estimates of the generalized steering vectors because a finite number of samples are used in estimating the cumulants. In Sections III-B and C, we worked with the generalized steering vector estimates one at a time to extract the bearings of coherent signals in each group separately, and when considering each group, we did not make use of the already existing generalized steering vector estimates of other groups. In this section, we show that this latter information can be used to improve the estimate of the generalized steering vector of each individual group. This is achieved by suppressing the undesired groups using a suitable beamformer so that the transformed received signal contains only the desired group. The same procedure is repeated for each group, and the transformed data is then processed as explained below. The transformations and subsequent processing can be implemented in parallel. The purpose of employing the beamformer is to minimize the cross-term effects in the cumulant estimates, which are present due to multiple groups.

Suppose that the generalized steering matrix $\boldsymbol{B}$ is estimated in the first step of EVESPA and that we are interested in the ith group arrival angles $(i = 1, \cdots, G)$. From the signal model, we have

$$\boldsymbol{r} = \boldsymbol{b}_i u_i(t) + \boldsymbol{B}_{u,i}\boldsymbol{u}_{u,i}(t) + \boldsymbol{n}(t) \tag{10}$$

where $M \times (G-1)$ matrix $\boldsymbol{B}_{u,i} \triangleq [\boldsymbol{b}_1, \cdots, \boldsymbol{b}_{i-1}, \boldsymbol{b}_{i+1}, \cdots, \boldsymbol{b}_G]$ and $(G-1)$-vector $\boldsymbol{u}_{u,i}(t) \triangleq [\boldsymbol{u}_1, \cdots, \boldsymbol{u}_{i-1}, \boldsymbol{u}_{i+1}, \cdots, \boldsymbol{u}_G]$. Both $\boldsymbol{B}_{u,i}$ and $u_{u,i}(t)$ are associated with the undesired groups.

Using the estimate $\hat{\boldsymbol{b}}_i$ obtained from the first step of EVESPA, we can find two beamformer vectors $\boldsymbol{w}_{i1}$ and $\boldsymbol{w}_{i2}$ such that $\boldsymbol{w}_{i1}^H\hat{\boldsymbol{B}}_{u,i} = \boldsymbol{w}_{i2}^H\hat{\boldsymbol{B}}_{u,i} = \boldsymbol{0}$, and $\boldsymbol{w}_{i1}^H\hat{\boldsymbol{b}}_i$ and $\boldsymbol{w}_{i2}^H\hat{\boldsymbol{b}}_i$ are nonzero. Two such vectors are obtained by picking any two of the left null space vectors of $\hat{\boldsymbol{B}}_{u,i}$. Since $\hat{\boldsymbol{b}}_i$ is independent of the columns of $\hat{\boldsymbol{B}}_{u,i}$, $\boldsymbol{w}_{i1}^H\hat{\boldsymbol{b}}_i$ and $\boldsymbol{w}_{i2}^H\hat{\boldsymbol{b}}_i$ are nonzero. Applying these beamformers to the received signal, we obtain two signals $\tilde{r}_1(t) = \boldsymbol{w}_{i1}^H\boldsymbol{r}(t)$ and $\tilde{r}_2(t) = \boldsymbol{w}_{i2}^H\boldsymbol{r}(t)$.[2] Ideally, these transformations suppress the contributions of all groups but the desired group $u_i(t)$. Hence, $\tilde{r}_1(t) \approx \boldsymbol{w}_{i1}^H\boldsymbol{b}_i u_i(t) + \boldsymbol{w}_{i1}^H\boldsymbol{n}(t)$, and $\tilde{r}_2(t) \approx \boldsymbol{w}_{i2}^H\boldsymbol{b}_i u_i(t) + \boldsymbol{w}_{i2}^H\boldsymbol{n}(t)$. Let $c_{i1} \triangleq \boldsymbol{w}_{i1}^H\boldsymbol{b}_i$ and $c_{i2} \triangleq \boldsymbol{w}_{i2}^H\boldsymbol{b}_i$ so that $\tilde{r}_1(t) \approx c_{i1}u_i(t) + \boldsymbol{w}_{i1}^H\boldsymbol{n}(t)$, and $\tilde{r}_2(t) \approx c_{i2}u_i(t) + \boldsymbol{w}_{i2}^H\boldsymbol{n}(t)$.

Defining the cumulant vector $\boldsymbol{v} \triangleq \text{cum}(\tilde{r}_1^*(t), \tilde{r}_1(t), \tilde{r}_1^*(t), \boldsymbol{r}(t))$ as the vector with the kth entry as $\text{cum}(\tilde{r}_1^*(t), \tilde{r}_1(t), \tilde{r}_1^*(t), r_k(t))$, an improved estimate of $\boldsymbol{b}_i$ can now be obtained to within a constant (which may be complex) from

$$\begin{aligned}\boldsymbol{v} &\approx \text{cum}\Big(c_{i1}^*u_i^*(t), c_{i1}u_i(t), c_{i1}^*u_i^*(t), \sum_{k=1}^{G}\boldsymbol{b}_k u_k(t)\Big)\\ &= \text{cum}(c_{i1}^*u_i^*(t), c_{i1}u_i(t), c_{i1}^*u_i^*(t), \boldsymbol{b}_i u_i(t))\\ &\quad + \text{cum}\Big(c_{i1}^*u_i^*(t), c_{i1}u_i(t), c_{i1}^*u_i^*(t), \sum_{k\neq i}^{G}\boldsymbol{b}_k u_k(t)\Big)\\ &= |c_{i1}|^2 c_{i1}^*\gamma_{4,i}\boldsymbol{b}_i\end{aligned} \tag{11}$$

where $\gamma_{4,i}$ is the fourth-order cumulant of the ith source, and we have used the independence of the source signals, the independence of the signals and the additive Gaussian-noise, and [**CP1**], [**CP3**], [**CP5**], [**CP6**] in [10]. This improvement method will be referred to as beamforming-based improvement 1 (BFBI1). A similar formulation was used in [3], where all signals but the desired one were assumed Gaussian, and therefore, they were suppressed by the cumulant operations.

In general, one can choose the beamformer vectors $\boldsymbol{w}_{i1}$ and $\boldsymbol{w}_{i2}$, which put nulls on all the undesired signals in $M-G+1$ ways. Let those vectors be $\{\boldsymbol{w}_{ik}\}_{k=1}^{M-G+1}$ and $\tilde{r}_k(t) \triangleq \boldsymbol{w}_{ik}^H\boldsymbol{r}(t)$. Then, further smoothing of the estimate of $\boldsymbol{b}_i$ is possible by taking the principal component of the rank-one matrix whose kth column is defined as $\text{cum}(\tilde{r}_k^*(t), \tilde{r}_k(t), \tilde{r}_k^*(t), \boldsymbol{r}(t)), k = 1, \cdots, M-G+1$. This improvement method will be referred to as BFBI2. Note that an estimate of $\boldsymbol{b}_i$ could also be obtained from the correlation $E\{\tilde{r}_k^*(t)\boldsymbol{r}(t)\}$ if there were no noise term in $\boldsymbol{r}(t)$.

Up to now, we assumed the undesired signals are suppressed perfectly so that we are left with only one source, and we could use the cumulant vector in (11); however, in practice, residual undesired signal terms are present in $\tilde{r}_1(t)$ and $\tilde{r}_2(t)$. In that case, the cumulant vector in (11) gives a weighted sum of generalized steering vectors of all the sources; therefore, it is better to use an ESPRIT-like formulation, as we did in the first step, which can handle multiple sources.

Let $\boldsymbol{d}_1 \triangleq [\boldsymbol{w}_{i1}^H\boldsymbol{b}_1, \cdots, \boldsymbol{w}_{i1}^H\boldsymbol{b}_G]$ and $\boldsymbol{d}_2 \triangleq [\boldsymbol{w}_{i2}^H\boldsymbol{b}_1, \cdots, \boldsymbol{w}_{i2}^H\boldsymbol{b}_G]$, where $\boldsymbol{w}_{i1}$ and $\boldsymbol{w}_{i2}$ are chosen as described above. Note that if perfect estimates of $\boldsymbol{b}_i$ were possible, all entries but $\boldsymbol{w}_{i1}^H\boldsymbol{b}_i$ of $\boldsymbol{d}_1$ and $\boldsymbol{w}_{i2}^H\boldsymbol{b}_i$ of $\boldsymbol{d}_2$ would be zero. Let us also define $\boldsymbol{C}_1 = \text{cum}(\tilde{r}_1^*(t), \tilde{r}_1(t), \boldsymbol{r}(t), \boldsymbol{r}^H(t))$ and $\boldsymbol{C}_2 = \text{cum}(\tilde{r}_1^*(t), \tilde{r}_2(t), \boldsymbol{r}(t), \boldsymbol{r}^H(t))$ as the $M \times M$ matrices whose (m, n)th elements, re-

[2] The reason why we have introduced $\tilde{r}_2$ will become clear later when we consider an ESPRIT-like formulation.

spectively, are $\text{cum}(\tilde{r}_1^*(t), \tilde{r}_1(t), r_m(t), r_n{}^*(t))$ and $\text{cum}(\tilde{r}_1^*(t), \tilde{r}_2(t), r_m(t), r_n{}^*(t))$. Using the notation $x(k)$ for the kth element of a vector $\boldsymbol{x}$, a simple expression for $\boldsymbol{C}_1$ is derived, as

$$\begin{aligned}\boldsymbol{C}_1 &= \text{cum}(\tilde{r}_1^*(t), \tilde{r}_1(t), \boldsymbol{r}(t), \boldsymbol{r}^H(t)) \\ &= \text{cum}\Bigg(\sum_{k=1}^{G} d_1(k)^* u_k^*(t), \sum_{k=1}^{G} d_1(k) u_k(t) \\ &\quad \cdot \sum_{k=1}^{G} \boldsymbol{b}_k u_k(t), \sum_{k=1}^{G} \boldsymbol{b}_k^H u_k^*(t)\Bigg) \\ &= \sum_{k=1}^{G} |d_1(k)|^2 \gamma_{4,k} \boldsymbol{b}_k \boldsymbol{b}_k^H = \boldsymbol{B\Lambda B}^H \end{aligned} \tag{12}$$

where $\boldsymbol{B} \triangleq [\boldsymbol{b}_1, \cdots, \boldsymbol{b}_G]$ and $\boldsymbol{\Lambda} \triangleq \text{diag}\{|d_1(1)|^2\gamma_{4,1}, \cdots, |d_1(G)|^2\gamma_{4,G}\}$, and we used **[CP1]**, **[CP3]**, **[CP5]**, **[CP6]** in [10]. Note that if one assumes perfect nulling, in which case all $d_1(k)$'s but $d_1(i)$ are zero, then $\boldsymbol{C}_1$ is theoretically rank one.

Similarly, $\boldsymbol{C}_2$ can be shown to be

$$\boldsymbol{C}_2 = \sum_{k=1}^{G} d_1(k)^* d_2(k) \gamma_{4,k} \boldsymbol{b}_k \boldsymbol{b}_k^H = \boldsymbol{B\Phi\Lambda B}^H \tag{13}$$

where $\boldsymbol{\Phi} \triangleq \text{diag}\{d_2(1)/d_1(1)^*, \cdots, d_2(G)/d_1(G)^*\}$.

By applying ESPRIT to (12) and (13), we can obtain an improved estimate of $\boldsymbol{b}_i$, which is then used in Steps 2 and 3 of EVESPA in the same way as explained earlier. This improvement method will be referred to as BFBI3. Note that because we are interested only in the part of $\boldsymbol{b}_i$ associated with the linear subarray in the second and third steps of EVESPA, we could use only the linear part of the data to improve the linear part of $\boldsymbol{b}_i$. This is accomplished by applying the same procedure explained here, in which $\boldsymbol{r}$ and $\boldsymbol{B}$ are replaced by their linear parts $\boldsymbol{r}_L$ and $\boldsymbol{B}_L$, respectively.

V. Experimental Results

In this section, we present results of some simulation experiments demonstrating our method.

A. Experiment 1: 14 Sensors, 20 Signals

We consider the array in Fig. 2. Each sensor in the array is a dipole antenna that has a response $\cos(\phi_j - \theta_i)$ to the jth signal, where ϕ_j is the arrival angle of the jth signal, and θ_i is the orientation of the ith dipole. The orientations of the dipoles are chosen arbitrarily as {95°, 85°, 87°, 92°, 90°, 90°, 90°, 90°, 90°, 90°, 90°, 90°, 90°, 90°}. There are four groups and five signals in each group. Each group contains a direct-path signal and several scaled and delayed replicas of the direct-path signal that represent the multipaths and "smart" jammers. In this experiment, there are 20 BPSK signals. Additive white Gaussian noise and a different SNR is assumed for each direct-path signal. The direction of arrivals and propagation constants of the signals within each group

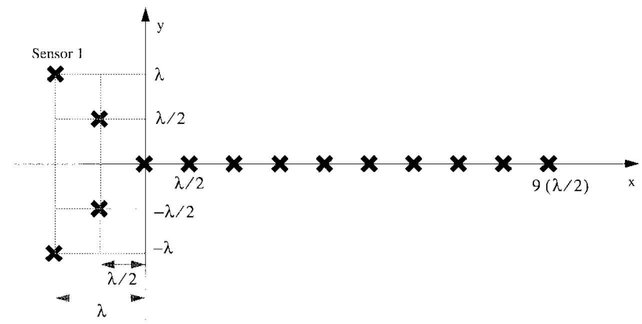

Fig. 2. Array configuration used in the first experiment. The antenna elements are dipoles oriented by the angles given in the text.

TABLE I
Sample Means and Standard Deviations of the Arrival Angle Estimates Based on the 100 Realizations of Experiment 1

	Groups							
	1		2		3		4	
Path	μ	σ	μ	σ	μ	σ	μ	σ
1	39.98	0.19	49.96	0.47	45.03	0.23	59.98	0.34
2	67.99	0.76	70.00	0.36	64.97	0.22	84.97	0.42
3	80.01	0.76	90.03	0.27	85.00	0.10	104.93	0.58
4	114.99	0.33	119.96	0.15	110.03	0.59	117.97	0.79
5	130.06	0.23	134.95	0.38	125.97	0.28	140.00	0.52

relative to the direct path and direct-path SNR's are chosen as follows, where unity propagation constants correspond to direct-path signals:

Group 1: DOA's: {40°, 68°, 80°, 115°, 130°}; propagation constants: $\{(0.2+0.8i), 1, (0.8-0.5i), (0.75+0.65i), (0.8-0.2i)\}$; direct-path SNR: 20 dB.

Group 2: DOA's: {50°, 70°, 90°, 120°, 135°}; propagation constants: $\{(0.9+0.3i), 1, (0.9-0.3i), (0.8+0.7i), 0.95\}$; direct-path SNR: 18 dB.

Group 3: DOA's: {45°, 65°, 85°, 110°, 125°}; propagation constants: $\{1, (0.8-0.7i), (0.7+0.7i), (0.65-0.8i), (0.9+0.1i)\}$; direct-path SNR: 18 dB.

Group 4: DOA's: {60°, 85°, 105°, 118°, 140°}; propagation constants: $\{(0.3-0.8i), (0.4+0.9i), (0.8+0.6i), (0.9+0.7i), 1\}$; direct-path SNR: 19 dB.

Assuming perfect knowledge of the number of sources and taking the right-most two dipoles in Fig. 2 as the guiding sensor pair, we applied our method to the scenario described above. We used 3000 snapshots to estimate the cumulant matrices described in the formulation of our method. Both forward and backward spatial smoothing with MUSIC were used in the second and third steps of our method. Fig. 3 shows the MUSIC spectrum for each coherent group obtained with our method for 100 runs of the experiment. The sharp peaks in the MUSIC spectrum give the arrival angle estimates. The actual arrival angles are also marked in Fig. 3. Observe that we are able to estimate all arrival angles, that our estimates appear to be consistent, and that our method is able to successfully separate close arriving angles belonging to signals in different groups.

In Table I, the sample means and standard deviations of the arrival angle estimates based on the 100 realizations are given.

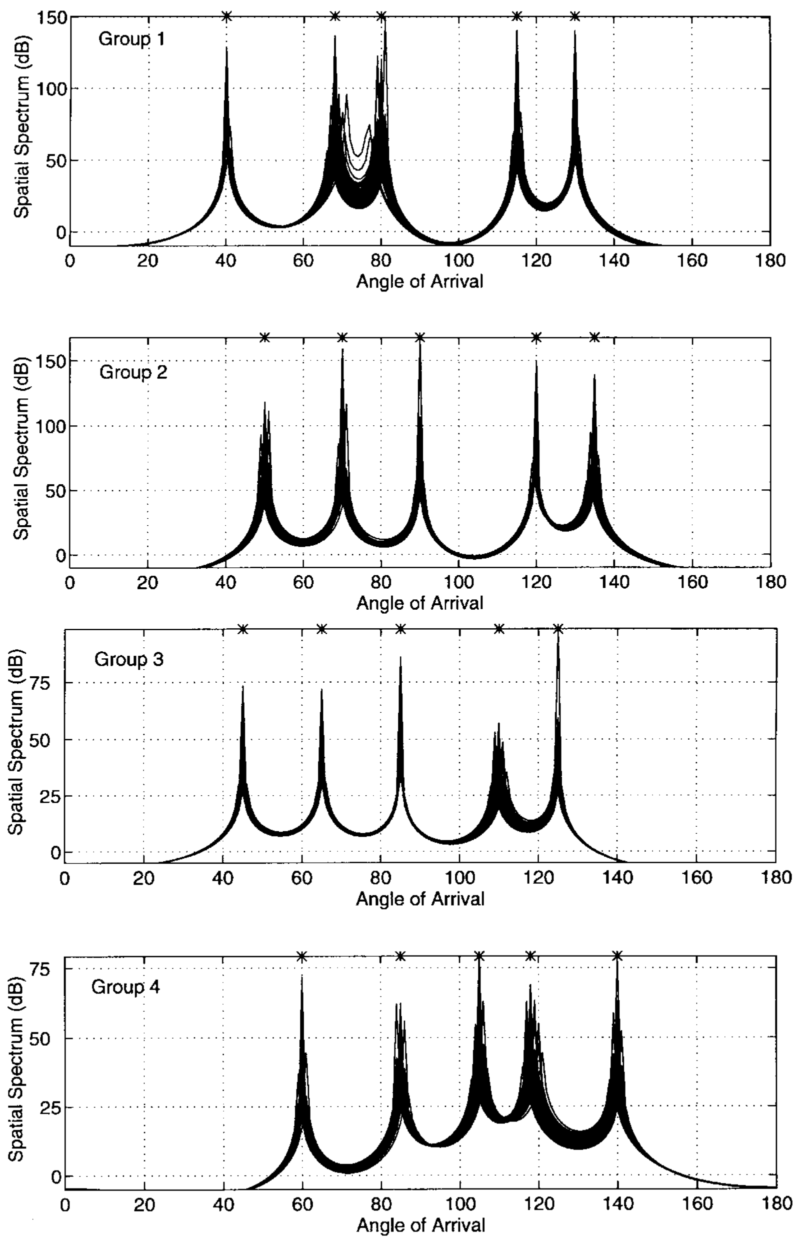

Fig. 3. MUSIC spectrum estimates for each coherent group obtained with our method for 100 runs of the first experiment. The actual arrival angles are marked with the symbol "*."

These values should be compared with those given above to see that our method performs well.

Note that we have a total of 20 signals and a ten sensor linear subarray; therefore, *covariance-based spatial smoothing fails since it can not resolve more sources than sensors*; therefore, there is no need to compare our results with covariance-based ones.

B. Experiment 2: Using Covariance Information

In this experiment, we show that projecting the generalized steering vector estimates onto the signal subspace obtained from the spatial array covariance matrix yields better angle estimates than those obtained from the basic version of EVESPA. This improvement method was proposed in Section IV-B.

For this purpose, we assumed the same signal scenario as in Experiment 1. We applied EVESPA for 100 different realizations of Experiment 1; for each realization, we also applied the method described in Section IV-B in order to get improved angle estimates, i.e., we projected the generalized steering vector estimates onto the signal space obtained from the spatial covariance matrix corresponding to the linear subarray. The number of snapshots was 2000. For both methods, we calculated the root-mean-square error (RMSE) for each angle estimate. The results are given in Table II. Observe that for low SNR's, our projection method gives better angle estimates than the basic version of EVESPA. As SNR increases, both versions tend to give equal performance. One concludes, therefore, that using the covariance information yields better results in low SNR environments.

C. Experiment 3: Improvement by BFBI3, 2 Groups

In this experiment, we substantiate our earlier claim in Section IV-C that the cross-term effects are reduced by sup-

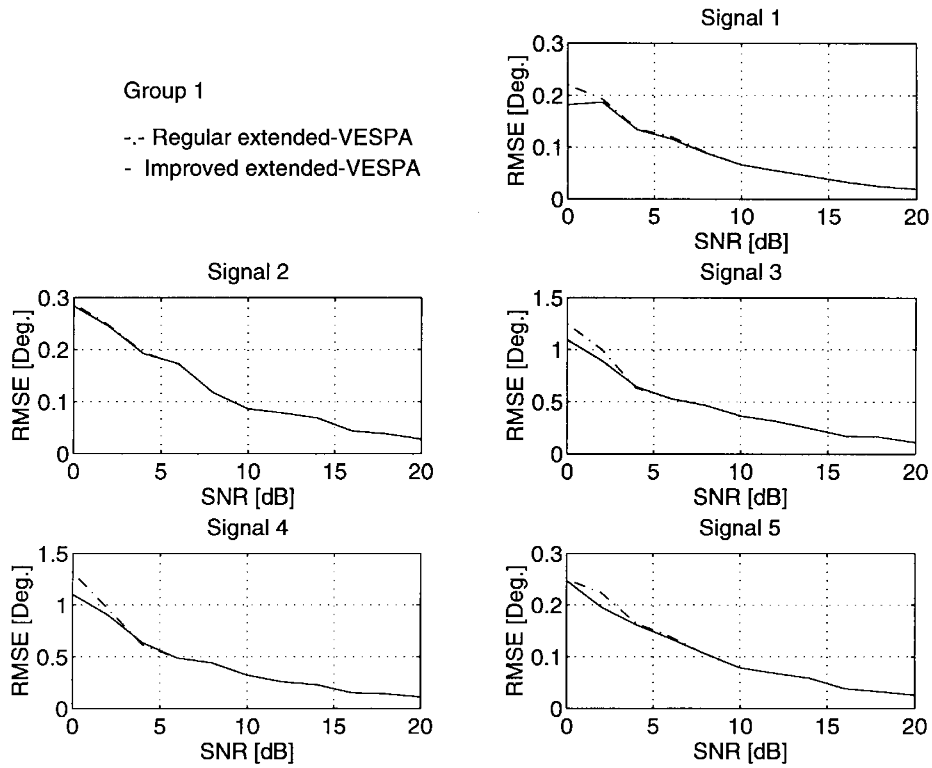

Fig. 4. Root-mean-square errors (RMSE's) for the arrival angle estimates of the second group obtained in Experiment 3 as a function of first group SNR. The ordering of the signals are the same as in the text.

pressing other groups when working with each group one at a time. We again consider the 14-element array in Fig. 2, but for simplicity, we assumed two groups, each containing five coherent signals, with the following propagation constants and arrival angles:

Group 1: DOA's: $\{45°, 70°, 90°, 100°, 120°\}$; propagation constants: $\{0.3 - 0.8i, 0.4 + 0.9i, 0.8 + 0.6i, 0.9 + 0.7i, 1\}$.

Group 2: DOA's: $\{50°, 65°, 80°, 93°, 110°\}$; propagation constants: $\{0.9 + 0.3i, 10.9 - 0.3i, 0.8 + 0.7i, 1\}$. The signals with unit propagation constants correspond to direct paths. We assumed circularly symmetric AWG noise, and 2500 snapshots were used. Although the direct path SNR of the second group was fixed at 10 dB, the first group SNR was variable and was increased by 2 dB steps in the range from 0 to 20 dB. For each value of the first group SNR, we performed a 100-run Monte Carlo experiment by running both EVESPA and its improved version BFBI3. Fig. 4 displays the RMSE's for the second group of arrival angles as a function of the first group SNR for both regular and extended-VESPA with BFBI3 improvement. The second group was assumed to be the desired one for BFBI3. As Fig. 4 shows, the RMSE curves for both versions of extended VESPA follow the same path up to 10 dB, after which, the RMSE performance of regular extended-VESPA deteriorates while the improved version gives better estimates. This observation supports our earlier claims: When the first group's signal powers are lower than those of the second group, cross terms in the second group's cumulant estimates due to the first group are negligible (see the region for SNR less than 10 dB in Fig. 4). Consequently, using BFBI3 to suppress the impact of first group does not reduce RMSE's of the second group's arrival angles. On the other hand, when the first group's signal powers are much higher than those of the second group (when SNR is greater than 10 dB), the cross terms present in the second group's cumulant estimates due to the first group are powerful. They result in poor sample estimates and, hence, degrade the RMSE performance of the regular extended-VESPA estimates. In this case, the improved version of extended VESPA suppresses the first group's signals and, therefore, reduces the cross terms as expected (see Fig. 4 for SNR greater than 10 dB). This, in turn, results in better cumulant estimates and, hence, better DOA estimates.

Fig. 5 displays the RMSE's for the first group arrival angles as a function of the first group SNR for both regular and extended-VESPA with BFBI3 improvement. The first group was assumed the desired one for BFBI3. As expected, the RMSE's decrease as the first group SNR increases. When the first group SNR is less than the second group SNR (the region for which SNR is less than 10 dB in Fig. 5), the improved method gives slightly better estimates. The reason is that in this region, suppressing the second group eliminates the cross terms in the first group's cumulant estimates due to the second group. As the first group SNR increases, the impact of cross terms due to the second group reduces; therefore, both methods give equally good estimates.

D. Experiment 4: BFBI1 versus BFBI3

In this experiment, we compare the beamforming improvement methods BFBI1 and BFBI3, which are described in Section IV-C in terms of mean-squared error performance. We also compare both methods to the regular version of EVESPA.

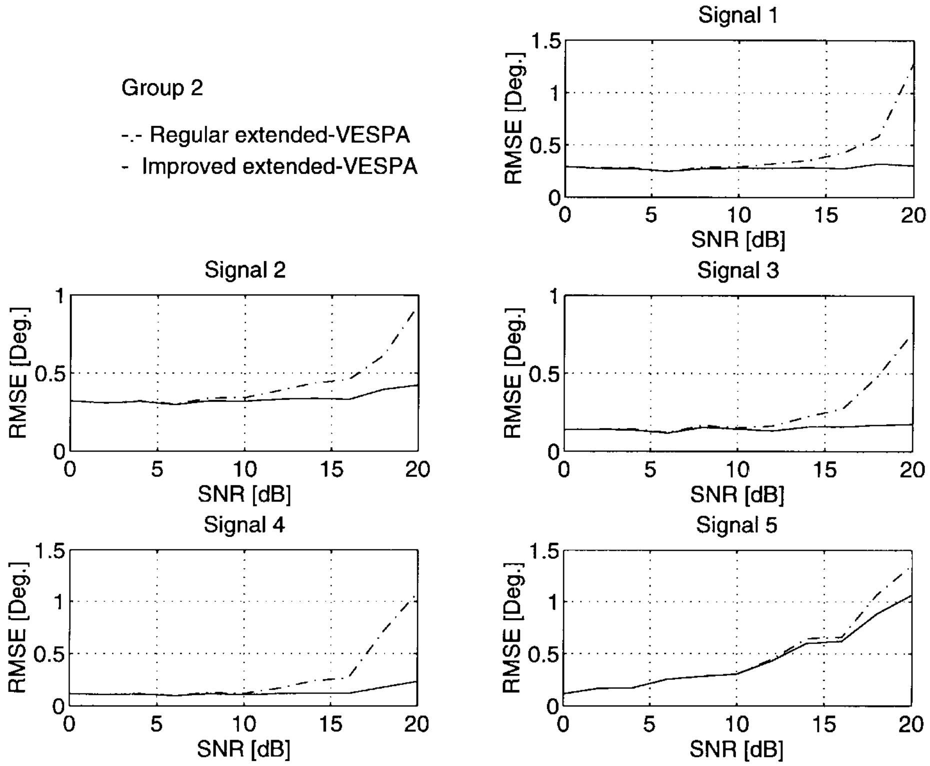

Fig. 5. Root-mean-square errors (RMSE's) for the arrival angle estimates of the first group obtained in Experiment 3 as a function of the first group SNR. The ordering of the signals are the same as in the text.

Note that the BFBI1 does not require the extra eigendecomposition that BFBI3 does and, hence, is computationally much simpler than BFBI3.

The signal scenario is as in Experiment 1. There are four groups each containing five signals. The direct path SNR for each group was increased simultaneously by 2 dB steps in the range -10 to 30 dB for all groups. For each value of SNR, we performed a 100-run Monte Carlo experiment by running both EVESPA and its two improved versions: BFBI1 and BFBI3. The RMSE's obtained by the three methods for the first group signals are plotted as a function of SNR in Fig. 6. Observe that the BFBI3 has the lowest RMSE among the three methods over a useful range of SNR values. In this experiment, the minimum required SNR for accurate estimation of DOA's with all of these three methods seems to be between -10 and 0 dB, below which neither of the three methods give reliable estimates since RMSE's are unacceptably high. For SNR greater than a threshold value, BFBI1 has about the same MSE performance as BFBI3, which is better than the performance of regular EVESPA. At an even higher SNR value, all three methods seem to have equal performances. These observations are easier to see from Fig. 7, which "zoom" in on the high SNR region of Fig. 6.

Conclusions to be drawn from this experiment are as follows: 1) Use BFBI1 for high SNR cases since it is computationally much simpler than BFBI3, and 2) for higher SNR's, neither cumulant-based beamforming method yields much improvement over regular EVESPA. Another interesting point to note is, as seen from Fig. 6, for some groups, below an SNR threshold, BFBI1 may yield even worse results than the regular EVESPA. This is because BFBI1 assumes that all groups, except the desired one, are perfectly suppressed, which is only true if the generalized steering vector estimates are estimated without error. For low SNR's, the sample cumulants, which are used to obtain the generalized steering vector estimates, are corrupted by high power additive noise; therefore, the vector-based improvement method may actually deteriorate the original generalized steering vector estimates. On the other hand, BFBI3 overcomes this problem by taking the principal component of a suitably defined cumulant matrix at the expense of computational load. Consequently, BFBI3 always yields the best MSE performance in the useful range of SNR values; therefore, it is recommended for low SNR's.

No simulations have been included for BFBI2 because BFBI3 is a better alternative than BFBI2 from an accuracy standpoint.

VI. Conclusions

We have shown that using cumulants, direction finding is possible in the coherent signals case. We have also shown that it is possible to detect more targets than sensors, which is an impossible task to accomplish using covariance-based subspace methods with arbitrary arrays, even in the case of *known* array response and *incoherent* signals.

Unlike some of the proposed cures for handling coherence, our method requires no array calibration, and unlike existing covariance-based spatial smoothing, for our method, the array does not have to be entirely linear. Only some part of the array must be linear, and the number of its elements determines the maximum number of resolvable signals in each coherent

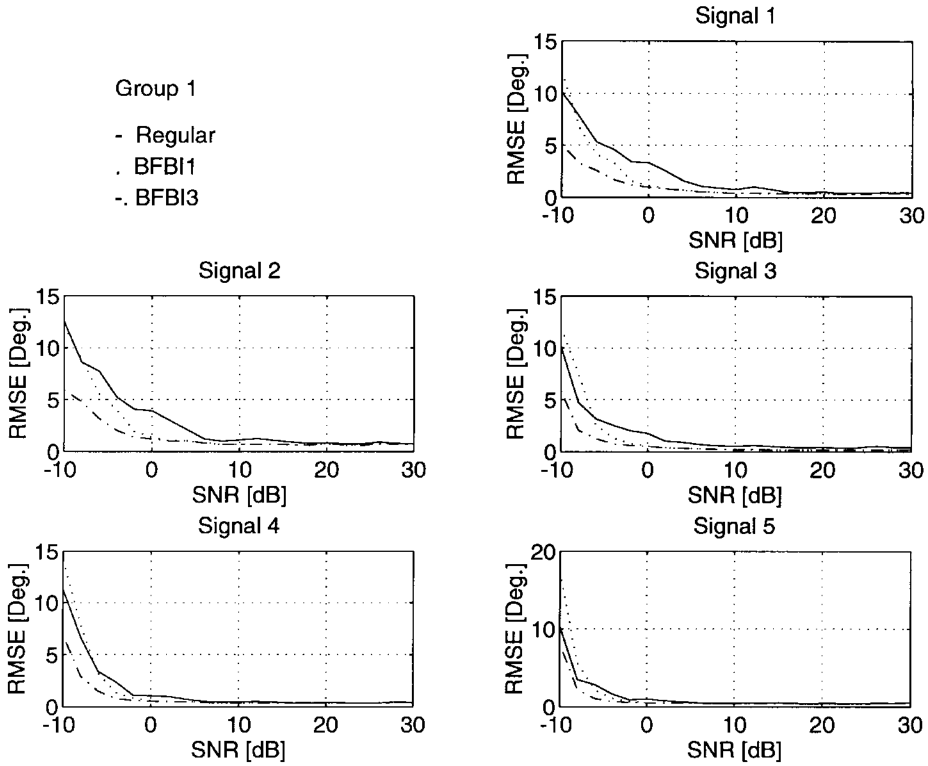

Fig. 6. Root-mean-squared errors (RMSE's) for the arrival angle estimates of the first group obtained in Experiment 4. BFBI1 and BFBI3 refer to the cumulant subspace-based and vector-based improvement methods, respectively. The ordering of the signals are the same as in the text.

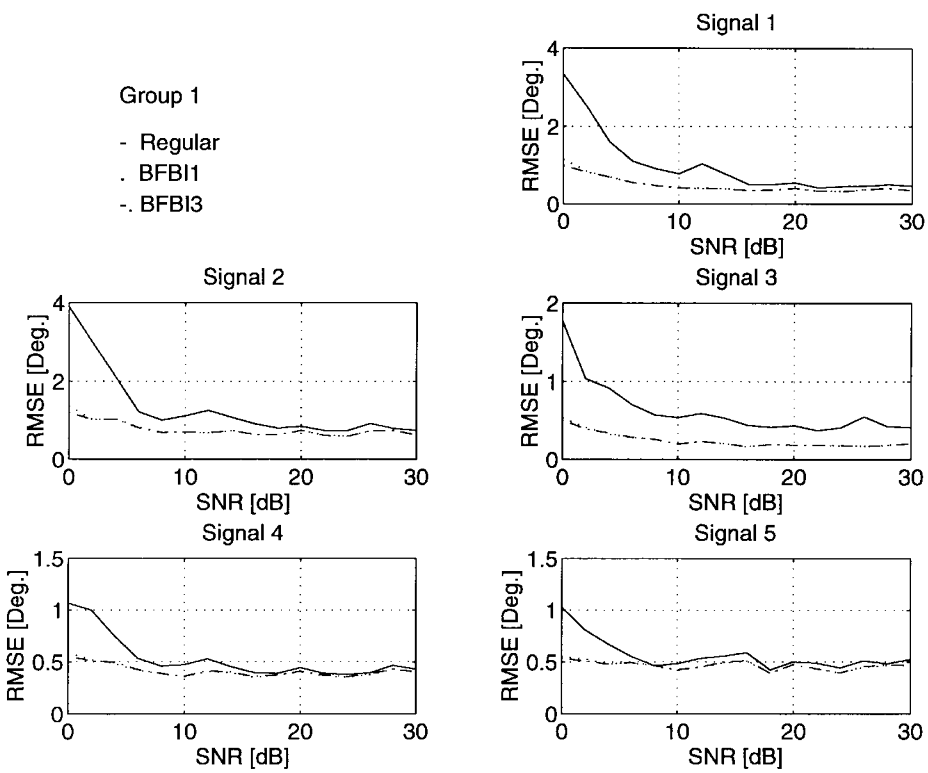

Fig. 7. High SNR region of Fig. 6.

group; the rest of the array may have arbitrary and unknown response and does not require calibration.

The entire array is fully exploited by our method, which results in a larger number of resolvable signals compared with the covariance-based spatial smoothing method. To be more specific, the total number of sensors determines the number of resolvable coherent groups. As shown in Section III-A, the presence of four arguments in the cumulants we are using

TABLE II
ROOT-MEAN-SQUARED ERRORS OBTAINED IN EXPERIMENT 2 FOR: (a) GROUP 1, (b) GROUP 2, (c) GROUP 3, AND (d) GROUP 4. VARIABLES $rmse_1$ AND $rmse_2$ REFER TO ROOT-MEAN-SQUARED ERRORS OBTAINED USING TWO DIFFERENT VERSIONS OF OUR DF METHOD, THE BASIC VERISON, , AND THE IMPROVED VERSION. THE LATTER IS OBTAINED BY PROJECTING THE GENERALIZED STEERING VECTOR ESTIMATES ONTO THE SIGNAL SUBSPACE OBTAINED FROM THE ESTIMATED SPATIAL COVARIANCE MATRIX OF THE LINEAR SUBARRAY, RESPECTIVELY. THE RESULTS WERE BASED ON 2000 SNAPSHOTS AND 100 REALIZATIONS AND ARE GIVEN FOR SNR LEVELS OF $[-10, -5, 0, 5, 10]$ dB

SNR	$Angle$	130	115	80	68	40
-10	$rmse_1$	4.08	7.90	12.11	7.49	12.04
	$rmse_2$	3.50	6.89	10.05	6.83	9.98
-5	$rmse_1$	2.38	2.35	3.24	2.67	3.07
	$rmse_2$	2.16	2.10	2.82	2.63	2.29
0	$rmse_1$	1.13	1.01	2.31	2.34	0.96
	$rmse_2$	1.01	0.99	2.30	2.33	0.81
5	$rmse_1$	0.75	0.69	2.21	2.08	0.75
	$rmse_2$	0.73	0.68	2.19	2.07	0.74
10	$rmse_1$	0.55	0.61	1.83	1.78	0.54
	$rmse_2$	0.54	0.61	1.83	1.77	0.53

(a)

SNR	$Angle$	135	120	90	70	50
-10	$rmse_1$	4.52	7.38	10.33	9.30	9.98
	$rmse_2$	2.81	7.73	9.60	8.58	8.36
-5	$rmse_1$	1.33	1.98	5.32	4.68	3.39
	$rmse_2$	1.19	1.82	4.31	4.01	2.86
0	$rmse_1$	0.83	1.05	1.74	1.77	1.18
	$rmse_2$	0.78	1.03	1.73	1.76	1.16
5	$rmse_1$	0.50	0.23	0.30	0.41	0.53
	$rmse_2$	0.49	0.22	0.29	0.41	0.52
10	$rmse_1$	0.44	0.20	0.25	0.36	0.42
	$rmse_2$	0.43	0.19	0.25	0.37	0.41

(b)

SNR	$Angle$	125	110	85	65	45
-10	$rmse_1$	5.17	7.37	6.52	9.45	8.49
	$rmse_2$	1.95	4.17	4.27	3.18	5.33
-5	$rmse_1$	1.09	1.96	1.60	1.11	1.37
	$rmse_2$	0.63	1.09	0.29	0.47	0.65
0	$rmse_1$	0.45	0.72	0.15	0.31	0.40
	$rmse_2$	0.44	0.74	0.16	0.32	0.40
5	$rmse_1$	0.33	0.68	0.11	0.11	0.24
	$rmse_2$	0.33	0.67	0.11	0.24	0.27
10	$rmse_1$	0.31	0.66	0.11	0.23	0.24
	$rmse_2$	0.31	0.67	0.11	0.23	0.24

(c)

SNR	$Angle$	140	118	105	85	60
-10	$rmse_1$	8.29	10.06	12.39	11.90	9.17
	$rmse_2$	3.29	5.52	6.47	5.66	4.48
-5	$rmse_1$	2.19	2.51	4.49	4.30	2.98
	$rmse_2$	1.65	2.47	1.93	1.76	1.29
0	$rmse_1$	1.08	1.46	1.87	1.69	1.16
	$rmse_2$	1.02	1.54	1.05	0.76	0.55
5	$rmse_1$	0.94	1.44	0.90	0.66	0.49
	$rmse_2$	0.89	1.37	0.88	0.66	0.49
10	$rmse_1$	0.89	1.30	0.81	0.66	0.49
	$rmse_2$	0.88	1.30	0.81	0.65	0.49

(d)

lets us first estimate the generalized steering vectors for each group. After estimating the generalized steering vectors, we use spatial smoothing as a postprocessing scheme on each individual generalized steering vector to find the directions of the signals in each group. Since covariances only have two arguments, a formulation to estimate the generalized steering vectors similar to Step 1 of our procedure is not possible for them; therefore, covariance-based methods can not handle signals on a group-by-group basis, which results in a reduced number of resolvable signals when they are used.

We have also developed several methods to improve direction-of-arrival estimates obtained by EVESPA. Among these methods, the subspace-based beamforming improvement method BFBI3 is found to offer the most significant improvement for low SNR's. For high SNR's, we suggest using extended-VESPA without the improvement methods.

EVESPA can replace existing covariance-based processing in a given array without requiring any modification in the associated hardware, provided the given array includes a linear subarray. Since independent groups are treated individually, processing can be parallelized to reduce the computing time.

ACKNOWLEDGMENT

The authors would like to thank the anonymous reviewers for their useful comments and suggestions.

REFERENCES

[1] A. Di, "Multiple source location-a matrix decomposition approach," *IEEE Trans. Acoust., Speech, Signal Processing*, vol. ASSP-33, pp. 1086–1091, Oct. 1985.

[2] M. C. Doğan and J. M. Mendel, "Applications of cumulants to array processing, Part I: Aperture extension and array calibration," *IEEE Trans. Signal Processing*, vol. 42, pp. 1200–1216, May 1995.

[3] ——, "Cumulant-based blind optimum beamforming," *IEEE Trans. Aerosp. Electron. Syst.*, vol. 30, pp. 722–741, July 1994.

[4] ——, "Applications of cumulants to array processing, Part II: Non-Gaussian noise suppression," *IEEE Trans. on Signal Processing*, vol. 42, pp. 1663–1676, July 1995.

[5] B. Friedlander and A. J. Weiss, "Direction finding using spatial smoothing with interpolated arrays," *IEEE Trans. Aerosp. Electron. Syst.*, vol. 28, pp. 574–587, Apr. 1992.

[6] E. Gönen, *Cumulants and Subspace Techniques for Array Processing*. Ph.D Dissertation, Univ. Southern California, Los Angeles, Dec., 1996.

[7] E. Gönen and J. M. Mendel, "Applications of cumulants to array processing—Part III: Optimum blind signal recovery for coherent signals," *IEEE Trans. Signal Processing*, this issue, pp. 2252–2264.

[8] E. Gönen, M. C. Doğan, and J. M. Mendel, "Applications of cumulants to array processing: direction finding in coherent signal environment," in *Proc. 28th Asilomar Conf. Signals, Syst., Comput.*, Asilomar, CA, 1994, pp. 633–637.

[9] F. Haber and M. Zoltowski, "Spatial spectrum estimation in a coherent signal environment using an array in motion," *IEEE Trans. Antennas Propagat.*, vol. AP-34, pp. 301–310, Mar. 1986.

[10] J. M. Mendel, "Tutorial on higher-order statistics (spectra) in signal processing and system theory: theoretical results and some applications," *Proc. IEEE*, vol. 79, pp. 278–305, Mar. 1991.

[11] H-H. C. Chiang and C. L. Nikias, "The ESPRIT algorithm with higher-order statistics," in *Proc. Workshop Higher Order Spectral Anal.*, Vail, CO, 1989, pp. 163–165.

[12] S. U. Pillai, *Array Signal Processing*. New York: Springer-Verlag, 1989.

[13] B. Porat and B. Friedlander, "Direction finding algorithms based on higher order statistics," *IEEE Trans. Signal Processing*, vol. 39, pp. 2016–2023, Sep. 1991.

[14] R. Roy and T. Kailath, "ESPRIT—Estimation of signal parameters via rotational invariance techniques," *Opt. Eng.*, vol. 29, no. 4, pp. 296–313, Apr. 1990.

[15] T. J. Shan, M. Wax, and T. Kailath, "On spatial smoothing for direction-of-arrival estimation of coherent signals," *IEEE Trans. Acoust., Speech, Signal Processing*, vol. ASSP-33, pp. 806–811, Aug. 1985.

[16] R. T. Williams, S. Prasad, and A. K. Mahalanabis, "An improved spatial smoothing technique for bearing estimation in a multipath environment," *IEEE Trans. Acoust., Speech, Signal Processing*, vol. 36, pp. 425–432, Apr. 1988.

[17] M. Zoltowski, and F. Haber, "A vector space approach to direction finding in a coherent multipath environment," *IEEE Trans. Antennas Propagat.*, vol. AP-34, pp. 1069–1079, Sept. 1986.

Egemen Gönen, for photograph and biography, see this issue, p. 2264.

Jerry M. Mendel (F'78), for photograph and biography, see this issue, p. 2264.

Mithat C. Doğan (M'94) was born on March 1, 1967 in Ankara, Turkey. He received the B.S.E.E. degree as a top-ranking senior from the Middle East Technical University (METU), Ankara, in 1988 and the M.S. and Ph.D. degrees in electrical engineering from the University of Southern California, Los Angeles, in 1989 and 1994, respectively.

He joined TRW Electromagnetic Systems Division (formerly ESL), Sunnyvale, CA, in 1994. He has been working on the design and implementation of blind signal separation algorithms for use in the next-generation signal collection systems. His major research interests are array signal processing, communication systems design/analysis, and applications of higher order statistics.

Dr. Doğan received TRW Chairman's Award for Innovation in 1995. He also received awards in recognition of academic excellence from the Scientific and Technical Research Council of Turkey (TUBITAK), including a NATO Science Fellowship for graduate studies. He is currently an honorary fellow of TUBITAK and a reviewer for several IEEE Transactions.